Dark side of the honeymoon: reconstructing the Asian x European rose breeding history through the lens of genomics

Thibault Leroy[1,2,3], Elise Albert[1,4], Tatiana Thouroude[1], Sylvie Baudino[5], Jean-Claude Caissard[5], Annie Chastellier[1], Jérôme Chameau[1], Julien Jeauffre[1], Thérèse Loubert[6], Saretta Nindya Paramita[5], Alix Pernet[1], Vanessa Soufflet-Freslon[1], Cristiana Oghina-Pavie[7], Fabrice Foucher[1], Laurence Hibrand-Saint Oyant[1]*, Jérémy Clotault[1]*

[1] Univ Angers, Institut Agro, INRAE, IRHS, SFR QUASAV, F-49000 Angers, France
[2] Department of Botany and Biodiversity Research, University of Vienna, Vienna, Austria
[3] GenPhySE, Université de Toulouse, INRAE, ENVT, Castanet Tolosan, France
[4] Syngenta Seeds SAS, Saint-Sauveur, France
[5] LBVpam-UMR5079, Université Jean Monnet Saint-Etienne, CNRS, Saint-Etienne, France
[6] Roseraie Loubert, Les Rosiers-sur-Loire, Gennes-Val-de-Loire, France
[7] Université d'Angers, CNRS, TEMOS, SFR CONFLUENCES, Angers, France

* These authors contributed equally to this work.

Corresponding author: Thibault Leroy, GenPhySE, Université de Toulouse, INRAE, INPT, INP-ENVT, Castanet Tolosan, France thibault.leroy@inrae.fr

ORCIDs:
Thibault Leroy: 0000-0003-2259-9723
Elise Albert: 0000-0001-5060-4505
Tatiana Thouroude: 0000-0001-7908-7353
Sylvie Baudino: 0000-0002-3367-172X
Jean-Claude Caissard: 0000-0001-7938-3101
Annie Chastellier: none
Jérôme Chameau: none
Julien Jeauffre: 0000-0001-6770-0552
Thérèse Loubert: none
Saretta Nindya Paramita: 0000-0003-4013-5009
Alix Pernet: none
Vanessa Soufflet-Freslon: 0000-0002-1264-7595
Cristiana Oghina-Pavie: none
Fabrice Foucher: 0000-0002-3693-7183
Laurence Hibrand-Saint Oyant : 0000-0002-7604-3811
Jérémy Clotault : 0000-0002-7678-1929

Summary

- Roses hold significant symbolic value in Western cultural heritage, often serving as a symbol of love and romance. Despite their ancient cultivation, the appreciation for the phenotypic diversity of roses emerged relatively recently, notably during the 19th century. This period is characterized by a remarkable expansion in the number of varieties, from around 100 to over 8,000, representing a golden age for roses.
- To trace the history of rose breeding in Europe and unveil genetic changes during this period, we gathered phenotypic and genetic data from 204 accessions. These included botanical roses and varieties cultivated between 1800 and 1910. Whole-genome sequences from 32 accessions were also included.
- Our analysis revealed a temporal shift in the genetic makeup, transitioning from a historical European to a near-Asian genetic background within a few generations. This shift was accompanied by a notable reduction in genetic diversity, attributed to the backcrossing with the less diverse Asian genepool, plus some genomic signatures of selection.
- We have generated the largest GWAS catalog for rose to date, offering a valuable resource for future breeding initiatives. We emphasize the critical importance of preserving ancient rose collections to safeguard diversity and ensure a sustainable breeding for the long term.

Introduction

The neolithic revolution, the move from nomadic hunter-gatherers to rooted agrarian societies, has profoundly changed the history of humankind (Diamond, 2002). This transition has allowed some populations to have larger food surpluses, favoring rapid population growth, a division of labor, technological innovations and, at the end, the establishment of dominant societies and colonizers (Diamond, 2005). Domestication is expected to generate drastic reductions in the effective population sizes due to the subsampling of the wild progenitor species and the selection pressures that have then further reduced population sizes, which have long been assumed to lead to sudden losses of diversity (Nei *et al.,* 1975; see Gaut *et al.,* 2015 for empirical evidences). Recent investigations thanks to ancient DNA samples, in sorghum in particular, are however more consistent with a long-term gradual, linear or nearly linear, decline rather than a rapid drop, requestioning in part this bottleneck scenario (Allaby *et al.,* 2019; Brown, 2019; Smith et al. 2019).

Unlike species domesticated for food production, the domestication of floral plants for aesthetic purposes is assumed to be far more recent, which can therefore even more question the existence of reductions of genetic diversity over these short periods of time. For most of the ornamentals, domestication indeed occurred in the last 500 years (Purugganan, 2022). Economically secure groups, especially the bourgeoisie in search of luxuries or aesthetic pleasure, have played a major role in this advent, leading to an exploding number of domesticated ornamental species, in such a way that ornamentals have been described

as outnumbering all other domesticated species combined today (Gessert, 1993, 2010; Chowdhuri & Deka, 2019). A typical example of this new passion for flowers in Western countries is tulips. Initially appreciated by Ottoman sultans and elites, the tulips imported to the Netherlands have led to a tulipmania, an irrational frenzy during the 17th century. Garden roses represent another emblematic example of domesticated flowers (Altman *et al.,* 2022), with a unique symbolic charge (Goody, 1993). Although rose domestication can be traced back as 5000 years BP (Altman et al, 2022), its golden age is assumed to be even more recent than tulips, dating back to the 19th century (Leus *et al.,* 2018).

Despite roses being cultivated since antiquity, both independently in China and the Mediterranean region, the number of varieties has long remained particularly limited. Thanks to considerable literature review efforts focusing on the 19th century, the history of a spectacular increase - by a factor 80 or so - in the number of rose varieties has however been revealed (~100 in 1800, 6,000-8,000 in 1900, 30,000-35,000 today; Marriott, 2003; Oghină-Pavie, 2021). The diversification during the 19th century is associated with crosses between the two previously isolated genetic backgrounds, the Asian and European gene pools, giving rise to a large number of horticultural groups, including hybrid tea roses from the late 19th century (Martin *et al.,* 2001). Hybrid tea roses are considered as the parents of the modern roses and are known to be phenotypically diverse, harboring traits that originate from Chinese roses, especially the capacity of recurrent flowering, a particularly targeted trait that led to an extension of the flowering period in Europe (Marriott, 2003; Soufflet-Freslon *et al.,* 2021). Large-scale genetic investigation based on more than a thousand varieties genotyped at 32 SSR markers have indeed identified 16 genetic groups, most associated with a gradient of population structure from a European (groups 1-3) to an Asian (group 9) genetic background during the 19th century, with more recent modern roses (>1914) exhibiting a close to Asian genetic structure (group 8, Liorzou *et al.,* 2016). Despite the progress made regarding the description of the genetic structure, there are many unknowns, including the number of generations of breeding, the levels of diversity and their evolution or the proportion of the respective European and Asian genomes. Similarly, while progress has been made regarding the description of genetic variation at some key genes of rose breeding, including *RoKSN* or *AP2*, two key genes controlling the duration of the blooming period and the doubling of the petal number, respectively (Iwata *et al.,* 2012; François *et al.,* 2018; Gattolin *et al.,* 2018; Soufflet-Freslon *et al.,* 2021), the genetic bases of most targeted traits in roses remain unknown.

Roses represent an excellent ornamental model to reconstruct the past history of breeding and investigate the genomic footprints of artificial selection. First, and most importantly, roses are maintained and reproduced through vegetative culture, in particular grafting, allowing the continuous maintenance of ancient varieties. This allows the phenotyping of roses that were bred at different periods of time in a single environment. In addition, it allows easy access to fresh material and therefore modern DNA from these varieties, without requiring expensive and challenging strategies such as the use of ancient DNA samples. Second, several reference genome assemblies are available for roses, in particular from the variety *Rosa chinensis* 'Old Blush' (Hibrand-Saint Oyant *et al.,* 2018; Raymond *et al.,* 2018), one of the four main ancient Asian roses used in plant breeding history (Liorzou *et al.,* 2016). Third, roses have relatively small genomes, around 500-550 Mbp - which for instance contrasts with the 34-Gbp of the tulip genome - allowing the resequencing of some rose accessions at affordable cost. Fourth, other molecular resources are available for roses, including a high density SNP array (68,893 markers, Koning-

Boucoiran *et al.,* 2015), making high resolution mapping and Genome-Wide Association Studies (GWAS) possible (SchulzDietmar *et al.,* 2016; Hibrand-Saint Oyant *et al.,* 2018). However, one challenge associated with the model is the variable ploidy level among roses, ranging from diploid to decaploid, even if most roses are either diploid or tetraploid. GWAS methods were initially developed for diploid models, but more recent developments, especially for polyploids (*e.g.* Rosyara *et al.,* 2016), provide new opportunities to uncover the genetic bases for important traits in roses. One additional difficulty associated with this model is the complexity of the genetic relationships in the *Rosa* genus, with a hundred or more wild species (Wissemann & Ritz, 2007; Debray *et al.,* 2021), for which approximately fifteen of them may have genetically contributed to present-day rose diversity.

In this study, we reconstruct the history of the rose garden breeding in Europe. To do so, we assembled a unique dataset, composed of large phenotypic data, genetic data from 204 roses genotyped with a 69k SNP array, plus whole-genome sequence data from 32 roses. The sequenced accessions are either botanical roses or varieties bred in Europe between 1800 and 1910, and include star varieties at that time. Botanical roses are considered as wild species, but they are maintained in rose collections and are assumed to be non-intentionally selected. By combining population genomics and quantitative genetic analyses, we (i) described the genomic makeup of the rose varieties, (ii) provided an approximate number of generations of selection, (iii) estimated the levels of genetic diversity and investigated their evolution throughout the period, (iv) identified potential footprints of artificial selection, and (v) performed the largest GWAS to date to uncover the genetic bases of many horticulturally important traits.

Materials and methods

Sampling & DNA extraction

All the 288 samples used for the Affymetrix array were collected in the 'Rose Loubert' rose collection and nursery (Roseraie Loubert, Gennes-Val-de-Loire, Pays de-la Loire, France) in summers 2020 and 2021, except for *Rosa* × *wichurana* and 'Old Blush', both collected in an experimental collection at INRAE (UE Horticulture, Angers, Pays de -la Loire, France).

Regarding the whole-genome sequences, each of the fifteen newly sequenced samples was chosen, based on its presumed importance during the 19th century (considered as "star varieties" based on extensive literature searches on historical catalogs of varieties; Cristiana Oghina-Pavie, personal communication) and the within-group diversity previously observed at 32 SSR markers (Liorzou et al., 2016). Fresh plant material was collected in the Roseraie Loubert in summer 2021, with the notable exception of 'Jin Ou Fan Lu', a cultivar that was previously collected by Shubin Li in China (Liorzou *et al.*, 2016). It should be noted that we had access to only a small part of the ancient roses, both because of the investigated collection, but also because a part of the ancient varieties have not been preserved down to this day. As a consequence, our sampling was potentially impacted by a conservation bias.

For each rose, 100 mg of leaves were collected and DNA was extracted from either lyophilised or fresh leaves using the Qiagen 96 Plant Kit (Qiagen, Hilden, Germany). DNA quality and quantity were checked with the Nanodrop technologies and Qubit kit prior to sending samples to the different facilities.

Genotyping and sequencing data

Genotyping was performed on 3*96-plates at the Gentyane facility (INRAE Clermont-Ferrand, France) using the Affymetrix Axiom technology. To further check the quality of the genotyping (see below), we included technical replicates (21 duplicate samples, as well as a triplicate one, shown in yellow in Table S1).

Regarding sequenced samples, library preparations and sequencing were performed at the Vienna BioCenter Core Facilities (VBCF, Vienna, Austria). For the library preparations, the facility used the Ultra II DNA kit for Illumina (New England Biolabs), which included an enzymatic shearing as a first step. Quality control was performed prior to sequencing. Quality control of the obtained NGS libraries was then assessed prior to the sequencing using the Fragment Analyzer technology. The 15 genotypes were then sequenced on a single NovaSeq SP flow cell (300 cycles, 2*150 reads). Demultiplexing was also performed by the VBCF facility.

Phenotyping

All phenotyping data were collected in the rose garden (Roseraie Loubert, Rosiers sur Loire, Gennes-Val-de-Loire, France). The number of petals was scored on at least two and at most five flowers. We used averaged petal counts across the different flowers.

For the recurrent blooming, the plants were scored in the rose garden every week during the blooming period (from spring to autumn) and this experiment was replicated during three years. We have previously developed a statistical method on the flowering curve using Gaussian mixture models and created indicators, as Reb.Mag for the magnitude of reblooming (for details, see Proïa et al. 2016). A value of 0 means that the rose flowers only in spring (once-flowering roses), the higher the value (above 0), the higher the reblooming capacity (see Supplementary Note 1). For the sake of clarity, the index shown in Fig. 1B corresponds to a simplified version, with values corresponding to three phenotypic classes (1: non-recurrent flowering, 2: partly recurrent, 3: recurrent flowering), an average value of the index across the three years of scoring was then computed for each individual.

For scent components, samples were collected during two years (2017 and/or 2018). From two to six flowers per sample and year (2017: mean=2.34, sd=0.78; 2018: mean=2.33, sd=0.81) were harvested around 10:00 am at stage 4 of flower development, as previously described (Bergougnoux *et al.,* 2007) and volatile compounds were extracted following Roccia *et al.* (2019). Per-genotype averaged values of each compound per year were used for all the analyses.

The black spot disease susceptibility was scored in the field over three years (2014, 2015, 2016). Each cultivar was scored, between July and September, depending on the development of disease and according to the scale indicated in Marolleau *et al.* (2020). The observed black spot symptoms were due to natural infection with natural inoculum of fungal strains. It should be noticed that we were scoring roses in the field, with present-day strains. The strains present at the time of breeding (*i.e.* 19th century) might have been different, including their virulence gene repertoires and aggressiveness factors.

Data analysis

The analyses performed in the manuscript are described below, considering (i) the analyses based on the SNP array and (ii) those on the whole-genome sequencing data. All the scripts

235 used have been made available on a github repository:
236 https://github.com/roseGWASbrowser/PopGen_GWAS_19thcentury_roses

237 ***1/ SNP array***

238 *Genotyping*

239 We used a two-round genotyping procedure to ensure highly accurate calls, in
240 particular regarding the GWAS analysis. First, we performed a QC analysis under Axiom
241 Analysis Suite based on all the genotypes (288). Based on this genotyping, four individuals
242 exhibited very low DQC (<0.25) and were excluded. Based on all the other individuals (with
243 DQC > 0.85, 284 samples), we generated a first genotype matrix with FitPoly (Voorrips et al.,
244 2011) assuming a ploidy=4 for all samples.

245 Given that roses are grafted, all samples with a close genetic proximity with the
246 rootstock cultivar used in the Loubert's rose garden were considered as sampling errors and
247 were excluded from the dataset (seven in total). In addition to these previously excluded
248 genotypes, we excluded seven additional genotypes with a DQC < 0.94 and a QC Calling
249 rate < 0.89, resulting in a dataset of 270 individuals. For this new dataset, we performed
250 detailed QC and then converted the output in a FitPoly format thanks to FitPolyTools
251 (version 1.1; unpublished R package by Roeland Voorrips). To take into account the variable
252 ploidy level between individuals, with the vast majority of the accessions used expected to
253 be either diploid or tetraploid, we generated a final genotyping matrix using FitPoly assuming
254 ploidy=4 for all individuals, which means that diploid individuals with heterozygous alleles are
255 generally expected to be called AABB. The rose SNP array targets 68,893 SNPs, with
256 probes for both strands, leading to a total number of 137,786 probes (for details, see Koning-
257 Bourcoiran *et al.,* 2015). After SNP filtering, we obtained a dataset of 92,007 probes,
258 corresponding to 56,467 of the 68,894 unique SNPs. Given all the difficulties associated with
259 the genotyping of the SNP array, especially in a species with a variable ploidy level, we
260 made the choice of using all probes satisfying our QC criteria in the subsequent analyses.
261

262 *QC checking and clone exclusion*
263 Given that roses are clonally propagated and used commercially worldwide, several varieties
264 can be registered under different cultivar names. In addition, spontaneous somatic mutants
265 (also called sport) exhibiting different traits (*e.g.* flower color or shape) are frequent in roses
266 and could have therefore been registered with two different names. To exclude potential
267 clones in the dataset that could bias our quantitative and population genomics analyses, we
268 computed the proportion of similar calls between all pairs of individuals and considered all
269 samples exhibiting a value higher than 0.965 as potential clones. To define this value, we
270 considered the observed distribution of the proportion of similar calls based on all pairwise
271 comparisons and the lowest observed value for a replicate of the analysis (0.973 for '*Persian*
272 *yellow*'), see Fig. S1 and Table S1 for a list. As a consequence, our "clone-corrected"
273 dataset contains 204 unique samples. All subsequent analyses are based on this dataset.
274

275 *Population structure*
276 We used the R package adegenet (Jombart, 2008) to explore the population structure
277 among the 204 individuals. We considered the whole set of 92,007 markers for the analysis.
278 We first used the df2genind (with ploidy=4) to generate the input files before using the
279 dudi.pca function of the adegenet package. PCA results were then plotted using both the
280 ggplot2 and ggrepel packages (Wickham, 2016; Slowikowski, 2023). To confirm the

population structure observed with the PCA, we also used faststructure (Raj *et al.,* 2014), with K ranging from two to five groups.

GWAS

Before performing GWAS analyses, we further filtered the dataset in order to exclude poorly informative markers. SNPs with a missing rate greater than 10% and/or a Minor Allele Frequency (MAF) < 0.05 were discarded, resulting in a set of 46,691 markers. GWAS was then performed with GWASpoly (Rosyara et al., 2016) for all traits using the kinship matrix and the structure inferred with a Principal Coordinates Analysis (dudi.pco, adegenet, Jombart, 2008). Considering both the tetraploidy and the absence of strong expectations regarding the additive *vs.* dominant effects of the genes for the studied traits, we considered all the potential models of gene action (*i.e.* general, additive, diplo-additive, diplo-general, simplex and duplex-dominant models, for details see Rosyara *et al.,* 2016). To explore the results, we first generated the qqplot and the Manhattan plot using R base, but we then generated linear or circular representations of the results under the R packages qqman (Turner *et al.,* 2018) or circlize (Gu *et al.,* 2014), respectively. In addition to the Manhattan plots, these circular views include density curves in order to identify some potentially interesting regions, even when the empirical background noise is high, generally associated with a general inflation of p-values (as observed with the qqplots). Given the number of traits analyzed, as well as the number of models explored for each, all the results were made available thanks to a dedicated website (https://roseGWASbrowser.github.io/).

2/ Whole-genome sequences

Mapping and calling

In total, 32 genotypes were analyzed, corresponding to a set of 17 rose sequences publicly available and to our 15 new sequences available on the Sequence Read Archive (SRA) under the BioProject PRJNA997103. Briefly, we used Trimmomatic (v.0.38, Bolger *et al.,* 2014) to remove adapters, trim and filter reads using the following set of parameters: LEADING:3 TRAILING:3 SLIDINGWINDOW:4:15 MINLEN:50. All trimmed reads were then mapped against a high-quality rose reference genome (Hibrand-Saint Oyant *et al.,* 2018) with BWA mem2 (v. 2.2, Vasimuddin *et al.,* 2019) using default settings. Most of the mapped data corresponds to paired ends reads but we also mapped single end reads (*i.e.* corresponding to unpaired after trimming). MarkDuplicates (Picard v. 2.20.7; Picard toolkit, 2019) was then used to remove potential PCR duplicates. Variant calling was performed on GATK4 (v.4.2.2.0, Poplin *et al.,* 2018), following the GATK best practices guidelines. In brief, we performed a first round of HaplotypeCaller to generate the GVCFs, followed by a CombineGVCFs and a GenotypeGVCFs with the "--all-sites true" option. Variants were then filtered with VariantFiltration, discarding variants with SOR>4.0, MQ<30, QD<2, FS>60, MQRankSum< -20, and ReadPosRankSum either <- 10 or >10.

Ploidy inference

The ploidy level of each sample was empirically determined by considering the observed allelic balance at heterozygous sites. Specifically, for each individual, we subsampled 2% of the total number of SNPs and then considered, for each individual, the heterozygous calls exhibiting a coverage greater or equal to 20 and then generated the per-individual density curves of the allelic balance based on all these SNPs. Because most of the polymorphisms

329 were expected to be rare in the population, we could observe the first neat peak to be near
330 f=0.25, 0.33 and 0.5 for tetraploids, triploids and diploids (see Fig. S2). Similar methods have
331 been developed over the last decade to empirically estimate the ploidy level (*e.g.* ploidyNGS,
332 Augusto Corrêa dos Santos *et al.,* 2017). To ensure that the inferred ploidy level was
333 sufficiently robust for our subsequent analyses, we checked the overall consistency of the
334 results with previous in-house estimates of the ploidy level (for details, see Liorzou *et al.,*
335 2016 and http://dx.doi.org/10.5281/zenodo.56704).
336
337 *Population structure & kinship*
338 Population genetic structure among the 32 varieties was performed using Principal
339 Component Analysis (PCA). Analyses were run on a set of 17,669 SNP, which was
340 generated by first randomly selecting 50,369 biallelic SNPs across the genome and then
341 pruning this set for linkage disequilibrium with plink (v1.90, parameters: "--index-pairwise 20
342 5 0.2"). We used the snpgdsPCA function from the SNPRelate R package (Zheng *et al.,*
343 2012) to generate the PCA. We then used ggplot2 (Wickham, 2016) to generate the final
344 plots. Given that the reference corresponds to an ancient Asian rose, we also empirically
345 checked that the observed population structure could not have been generated by a strong
346 mapping bias (Fig. S3). As a control of the population structure observed using PCA, we also
347 used faststructure (Raj *et al.,* 2014) on the same 50k SNP set. To do so, we first used plink
348 (v2.00, Purcell *et al.,* 2007) to generate the input files and then inferred the population
349 structure for K=1 to K=6. Barplots of the inferred individual ancestry memberships were also
350 generated using ggplot2.
351
352 We performed a family relationship inference by estimating kinship coefficients under KING
353 (Manichaikul *et al.,* 2010) based on the whole SNP set (77,862,879 filtered SNPs). The initial
354 objective of this analysis was to ensure that no clones were present in our sequencing
355 dataset (see also above). But given that KING is able to infer relationships up to the third-
356 degree (*i.e.* great grandparents and great grandchildren, first cousins, or similar), we used
357 KING to infer some potential family relationships. We first generated the input files with plink
358 (v2.00) and then estimated kinship coefficients. Kinship values higher than 0.354 correspond
359 to clones, while coefficients coefficients within the intervals [0.177, 0.354], [0.0884, 0.177],
360 and [0.0442, 0.0884] correspond to 1st-degree, 2nd-degree, and 3rd-degree relationships,
361 respectively. Based on our data, KING was able to infer a remarkably high number of family
362 relationships among our dataset composed of "star varieties" (see results). As a
363 consequence, we used the R package igraph (Csárdi & Nepusz, 2006) to generate a
364 comprehensive network based on all the inferred family relationships.
365
366
367 *Nucleotide diversity estimates*
368 As compared to population structure and kinship inferences, estimates of diversity are highly
369 dependent on the final quality of the SNP set. To ensure unbiased estimates, we used the
370 filtered set of SNPs based on the 32 samples (77,862,879 filtered SNPs) to perform a Base
371 Quality Score Recalibration (BQSR) on the 19 retained samples, as recommended by GATK
372 in the absence of a highly-reliable SNP catalog for the focal species. Then, we used GATK's
373 ApplyBQSR function. HaplotypeCaller was then performed assuming the inferred ploidy (see
374 previous section) using option "--ploidy", before using CombineGVCFs, GenotypeGVCFs
375 and VariantFiltration as previously described to generate a final SNP set of 54,481,222
376 filtered SNPs. We then reconstructed whole-genome fasta sequences based on the

377 complete VCF (vcf with variant and non-variant positions; to know more about the
378 importance of using non-variant positions, see Korunes & Samuk, 2021) following Leroy and
379 collaborators (2021a, 2021b). The approach was adapted to the rose specificities to
380 reconstruct up to 4 sequences per individual, by explicitly considering the inferred ploidy
381 (per-individual number of alleles in the GT field). Briefly, the pipeline reconstructs the
382 sequence by considering the coverage at each position. All positions that are not in between
383 the 5th and 95th centiles of the individual coverage, as well as those with coverage lower
384 than 3 were hard-masked in the reconstructed sequences. For positions satisfying the
385 coverage criteria, the reference allele is added to the reconstructed sequences, except at
386 PASS positions, where alleles are added according to the genotyping calls (*i.e.* the GT field).
387 Triallelic (or more) variants were discarded. Similarly, indels were ignored to keep the
388 sequence length the same across individuals and therefore obtain perfectly aligned
389 sequence blocks. Nucleotide diversity and Tajima's D were then computed on non-
390 overlapping 100-kbp sliding windows following Leroy *et al.* (2021a) for each group, based on
391 the individuals falling in the four following groups: ancient Asian, ancient European, early
392 European x Asian and hybrid tea roses (Table S2). Botanical roses were not included in this
393 part of the study because their population structure is not consistent with a single group. A
394 Reduction of Diversity (RoD) index was computed by $1 - \frac{\pi Group1}{\pi Group2}$, with *Group1* and *Group2*
395 corresponding to hybrid tea roses and ancient European, respectively, for a comparison
396 aiming at estimating the evolution of the diversity in hybrid tea roses as compared to the
397 ancient European samples. A positive value of the RoD index therefore indicates a net
398 reduction of the nucleotide diversity between the two groups. Circular visualization was
399 generated using the R package circlize (Gu *et al.,* 2014).
400
401 *Diagnostic alleles*
402 For each filtered SNP among the final list of 54,481,222 SNPs, allele frequencies of the four
403 groups were computed directly based on the filtered joint vcf thanks to a home-made script
404 (script_freqgroup4localancestryprop.py), which was made available on the github repository
405 (https://github.com/roseGWASbrowser/PopGen_GWAS_19thcentury_roses). Given that the
406 number of genotypes available per group is limited, allele frequency was only computed if
407 the number of missing alleles was lower or equal to 4 (*i.e.* corresponding to a maximum of 1
408 tetraploid individual or 2 diploid individuals without genotyping calls). We then subsampled
409 SNPs exhibiting diagnostic alleles, *i.e.* an allele frequency of the reference allele of 0 and 1
410 in one group and in the other. In this specific example, all diagnostic SNPs identified - at the
411 notable exception of 2 SNPs that were subsequently excluded - exhibit an allele frequency of
412 0 in the European and of 1 in the Asian group. Indeed, all the raw sequencing data were
413 mapped against the genome of an ancient Asian genotype ('Old Blush'; Hibrand-Saint Oyant
414 *et al.,* 2018). Consequently, the reference alleles are expected to be more associated with
415 the ancient Asian background. The match is almost perfect here given that we also used the
416 'Old Blush' variety as a member of the ancient Asian group in our study. As a consequence,
417 all diagnostic alleles are expected to have an allele frequency of 1 in the ancient Asian group
418 and, consequently, 0 in the ancient European group. In total, we identified 170,637
419 diagnostic SNPs on our sampling. Diagnostic SNPs are observed on all chromosomes
420 (Table S3). Importantly, the diagnostic SNPs are based on our limited panel of varieties.
421 Consequently, all are not expected to be truly diagnostic based on a larger panel.
422 Local ancestry of early European x Asian or hybrid tea groups was then estimated by
423 computing the median of the observed allele frequencies at diagnostic markers. Estimates

were based on non-overlapping 100-kbp sliding windows spanning the whole genome for windows containing at least 5 diagnostic SNPs.

Local footprints of selection

To know more about the genomic regions targeted by 19th century breeders, we identified regions that could be consistent with selective sweeps. One limitation associated with the model is the recent history of the rose breeding and the associated limited number of generations of recombination (see results). As a consequence, explicit selective sweep methods could not be used here to identify potential footprints of selection. As an alternative, we identified regions simultaneously exhibiting the lowest π, the most negative Tajima's D and the highest RoD values. Given that this strategy does not fully circumvent the problem of the lack of generations of recombination, we have decided to focus our detection on hybrid tea roses, the latest group in the history of breeding among those investigated in this study, and therefore expected to have experienced the highest number of generations of recombination, in order to deliver more interpretable results. We considered two sets of candidate windows. The stringent set corresponds to windows falling in the last centile of the three metrics supporting a potential selective sweep (*i.e.* bottom 1% of nucleotide diversity and Tajima's D values, top 1% of the RoD comparing hybrid tea roses with either Ancient European or Ancient Asian), and a less stringent set considering the last five centiles (Table S4).

Results

19th century: directed or unintended evolution of some key rose traits

Asexual rose propagation through grafting or cutting allows the maintenance of ancient roses in gardens and therefore the direct comparisons of phenotypes obtained at different periods of the breeding history. We explored the phenotypic variation of a large collection of botanical and ancient accessions, representing more than 200 roses bred between 1800 and 1910 (Fig. 1A), a period which is considered as the golden age for rose breeding. In this study, we investigated about 30 traits in 200+ varieties, including several presumably crucial traits for breeding, such as the blooming period, the color and number of petals, the number of prickles, the resistance to black spot disease, plus some flower and plant architecture phenotypes (Fig. 1B). A particularly massive effort was made to analyze the floral scent by quantifying the volatile compounds of the collection using a GC-MS strategy, including the 2-phenylethanol and the geraniol, which represent two main components of the floral rose scent (Spiller *et al.,* 2010; Magnard *et al.,* 2015; Roccia *et al.,* 2019; Caissard *et al.,* 2022).

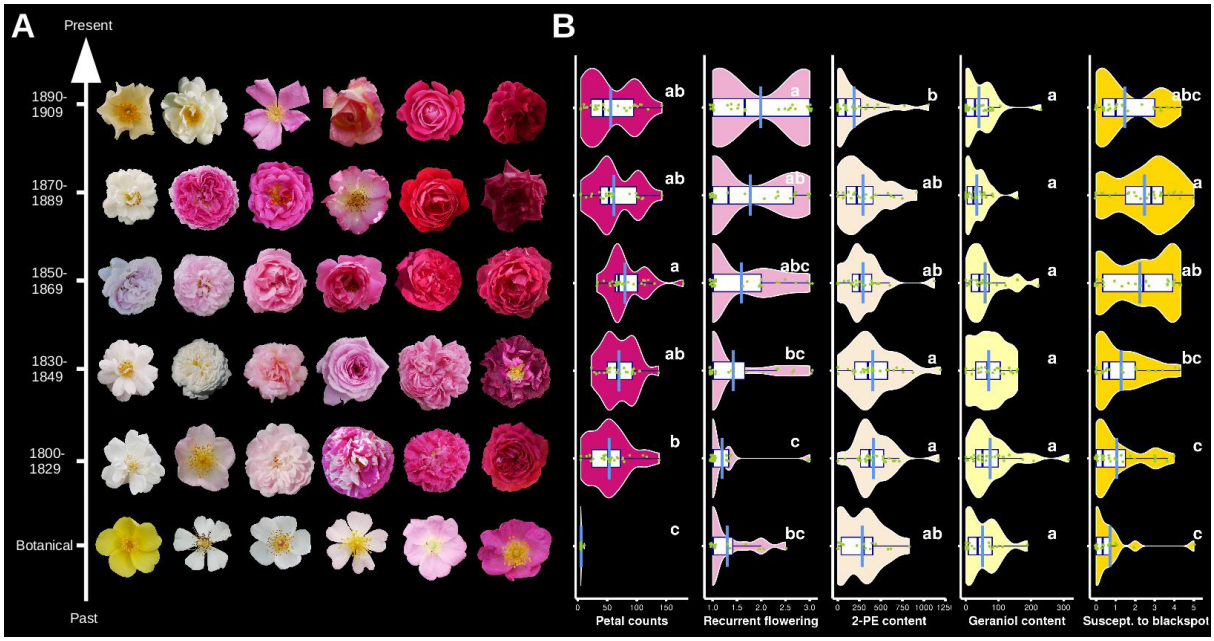

Figure 1: Main phenotypic changes along the 19th century plant breeding history. A. *Pictures highlighting the phenotypic variation of flowers at different periods of the rose breeding history among the different accessions used in this study. Pictures were taken by T. Leroy in the Loubert rose collection in 2021 and 2022 and selected to be representative regarding the number of petals and the variation of colors observed among all the varieties of a given period. Pictures are not to scale.* ***B.*** *Phenotypic variation for some of the studied traits: number of petals (dark pink), recurrent flowering (light pink, estimated by an index), scent components (2-phenylethanol and geraniol contents, light beige and light yellow, respectively) and susceptibility to black spot disease (yellow). Averages are shown with light blue lines. Tukey's honestly significant difference (HSD) tests at α=0.05 are indicated with letters.*

Among all these traits, those associated with flowering are expected to be the main target of selection during the 19th century, including the production of roses containing tens of petals and the ability to have an extended blooming period. Most botanical accessions indeed produce flowers containing only five petals (Fig. 1B) and during a limited period of time in spring. Based on our sampling, the mean number of petals has strongly increased during the first half of the 19th century (including roses with up to 210 petals), emphasizing the importance of selecting for this trait at the beginning of the 19th century. From 1870, the trend reversed with a reduction of the mean number of petals. This suggests either the relaxation of this selective pressure for an increasing number of petals or a change in aesthetic preferences. The latter hypothesis appears the most likely from a historical perspective, for several reasons: (i) varieties with up to 60 petals are nowadays preferred to obtain high-centered buds when the rose flowers are opened, (ii) the rosomania had led to the establishment of rose connoisseur communities from 1880, interested by new targets of selection, including wild-like phenotypes such as single flower (five petals) and spring roses (Oghina-Pavie, 2020). Indeed, at the end of the 19th century, additional rose species were used as breeding materials, such as *R. multiflora* and *R. rugosa*, with single flower and non-recurrent blooming phenotypes. Selection for roses with the ability to rebloom (recurrent blooming) is expected to represent another main historical target of the rose breeding. Phenotypic variation at this trait indeed supports a relatively constant increase of the repeat-flowering phenotype based on our rose collection, with a progressive increase of the mean of the recurrent blooming index during the 19th century (Fig. 1B).

A main criticism associated with modern roses is the popular impression of a reduction of the flower fragrance. Based on our collection of roses, a slight reduction was indeed observed during the 19th century based on the mean contents of both 2-

501 phenylethanol and geraniol, two main components of the rose scent. Changes during this
502 period are however either weakly significant or non-significant depending on the
503 components, owing mainly to the large observed variance among roses of each period (Fig.
504 1B).
505 Temporal changes in the resistance to *Diplocarpon rosae*, the pathogen responsible
506 for black spot disease - one of the most serious diseases on garden roses today -, were also
507 investigated. As compared to the previous examples, resistance to black spot was likely not
508 directly selected by breeders at that time since rose growers started to show interests for
509 *Diplocarpon rosae* (also called *Marssonina* ou *Marsonia rosae* Briosi & Cavara) at the
510 beginning of the 20th century (Ducomet, 1903; Cristiana Oghina-Pavie, personal
511 communication), even though today the resistance to this fungal pathogen represents one of
512 the main breeding targets. Botanical roses from our collection exhibit exceptional resistance
513 levels to *D. rosea* (*i.e.* low susceptibility score) but this resistance has progressively
514 plummeted during the rose breeding history, at least until 1890 (Fig. 1B, see also Fig. S4),
515 which therefore questions the origin of this erosion of resistance (loss of resistance alleles,
516 evolution of the pathogen, etc). Yellow and orange-colored roses are often suspected by
517 breeders to be more susceptible to black spot, hypothetically leading to a trade-off between
518 colors and resistance for breeders. No significant differences in susceptibility were however
519 observed between varieties with different main color petals (Fig. S5). The hypothesis
520 regarding the higher susceptibility of yellow flower varieties remains open since our sampling
521 is biased toward pink and white flowers, largely underrepresenting the genotypes with yellow
522 flowers, mostly because roses with yellow- or orange-colored flowers were relatively rare
523 during the 19th century (Leus *et al.,* 2018).
524
525 **A rapid shift from a European to an Asian genetic background**
526
527 The same large collection of rose varieties was genotyped at 68,893 SNPs using the
528 Rose Genotyping Array (WagRhSNP Axiom Array, Koning-Boucoiran *et al.,* 2015), a SNP
529 array developed from modern cut and garden roses. After the removal of clonal genotypes, a
530 final set of 204 rose varieties was used for the subsequent analyses (see Materials and
531 methods, Fig. S1 and Table S1). The first axis of a Principal Component Analysis (PCA)
532 explains more than a fifth of the total variance (21.4%) and isolates the two ancient genetic
533 backgrounds: an Asian one (in yellow) and an European one (in blue, Fig. 2A). The whole
534 dataset forms a gradient of population structure between the two backgrounds, which is
535 consistent with the frequent crosses between European and Asian roses throughout the 19th
536 century. The second axis isolates some samples, including most of the botanical samples,
537 from the Asian-European gradient. This population structure is mostly consistent with a
538 previous report based on the genotyping at 32 microsatellite markers of an even larger
539 collection of varieties and the identification of 16 genetic groups (Fig. 2A, Liorzou *et al.,*
540 2016).
541 Independently from this first dataset, we resequenced 15 varieties and collected publicly
542 available rose genomes to generate a dataset of 32 samples, composed of ancient Asian,
543 ancient European, early European x Asian, hybrid tea and botanical samples (Table S2).
544 After joint-genotyping and SNP filtering, we generated a dataset of 77,862,879 filtered SNPs
545 on the 32 samples. PCA based on a LD-pruned set of 17,669 variants among 50,369
546 randomly selected SNPs (Fig. 2B) is consistent with an Asian-European gradient of
547 population structure, as previously identified with the SNP array (Fig. 2A). The proportion of
548 variance explained by the first axes is however lower based on the sequencing data, likely
549 due to SNP ascertainment bias associated with the design of the array, since the SNP set
550 was established based on the analysis of more modern varieties, therefore emphasizing
551 more on the European-Asian gradient (*i.e.* the axis 1). Based on the WGS data, some axes

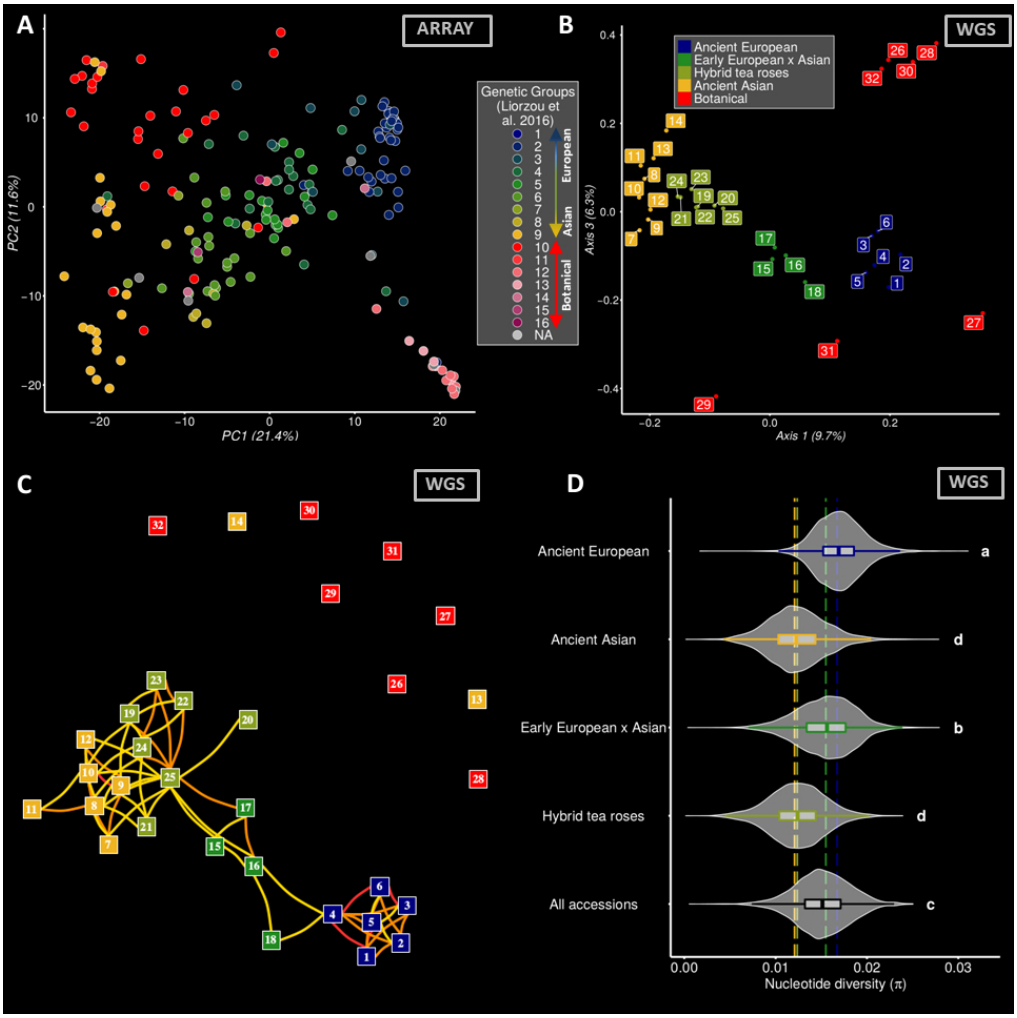

Figure 2: Population structure and levels of genetic diversity in several rose groups used in the 19th century rose breeding history. A. *Population structure of the 204 varieties genotyped with the rose SNP array based on the two first axes of a Principal Component Analysis (PCA). To check the consistency with previous works, the membership of the samples to one of the 16 genetic groups defined by Liorzou and collaborators (2016) based on the analysis of SSR markers are shown (for details, see Liorzou et al., 2016). Roses with ancient European and ancient Asian backgrounds are shown in blue and yellow, respectively (typically corresponding to groups 1-3 and 9, respectively; see also Fig. S6 and S7).* ***B.*** *Population structure based on the whole-genome sequences used in this study. Axes 1 and 3 of a Principal Component Analysis (PCA) based on a random sampling of 50k SNPs. Ancient European, ancient Asian, early European x Asian, hybrid tea varieties and botanical accessions are shown in blue, yellow, green, khaki and red, respectively. Results from other components as well as more detailed information about the cultivar IDs are shown in Figs. S8 and Table S2, respectively (but see also Fig. S9).* ***C.*** *Network of the relationships inferred based on the kinship coefficients estimated under KING based on the whole SNP set of 77,862,879 SNPs. First-, second- and third-degree relationships are represented with red, orange and yellow lines, respectively. See Table S2 for a correspondence table between accession numbers and cultivar IDs.* ***D.*** *Genetic diversity estimates based on the different groups. Distribution of the nucleotide diversity levels based on non-overlapping 100 kb sliding windows spanning the genome (each dot corresponds to a window). Genomic windows on chr00 are not included. For ease of comparison, a vertical line is shown representing the mean π value per group.*

575 can be built due to a single botanical individual (*e.g.* axes 2 and 4, Fig. S8), suggesting that
576 a large proportion of the diversity is indeed only present in the botanical accessions.
577 Family relationships were then inferred using KING (Manichaikul *et al.,* 2010) based
578 on the pairwise kinship values calculated on the sequencing data. Among the 32 samples,
579 only a few individuals are not connected to at least another individual of the dataset through
580 a third degree relationship (*i.e.* kinship coefficient > 0.0442) (Fig. 2C). These individuals
581 correspond to all botanical samples, plus two ancient Asian samples (*R. odorata gigantea*
582 and *R. chinensis spontanea,* numbers 13 and 14 in Fig. 2C, respectively). The rest of the
583 individuals are connected through a large network, linking the ancient European and the
584 ancient Asian backgrounds through the early European x Asian and hybrid Tea varieties
585 (Fig. 2C). This result is remarkably consistent with the expected history of selection during
586 the 19th century, with (1) the intercrossing of the Asian genepool with the European one in
587 the European breeding practices, (2) leading to the obtention of early European x Asian
588 varieties, and (3) the backcrossing of these early hybrids with the ancient Asian genepool to
589 obtain the hybrid tea varieties. Obtaining such a network with a so limited number of
590 samples, and without integrating prior knowledge about the potential pedigrees, suggests
591 that the selection was based on a quite narrow diversity, in terms of the number of varieties
592 used. In addition, it suggests that the number of generations of selection was also very
593 limited. Hybrid roses from the 19th century are indeed connected to Asian and European
594 gene pools by less than 10 generations of breeding (Fig. 2C).
595 SNPs with diagnostic alleles between the ancient Asian and ancient European
596 samples were then identified, resulting in a subset of 170,637 diagnostic SNPs (Fig. S10). At
597 these markers, the early European x Asian samples remarkably have a 1:1 ratio, *i.e.* an
598 almost equal share between the two gene pools (50.9% and 49.1% of Asian and European
599 alleles, respectively). One might propose that this 1:1 ratio implies that all early European x
600 Asian samples used in the study are first-generation (F1) hybrids between the ancient Asian
601 and European groups of samples. However, detailed analyses at the individual level are
602 inconsistent with this hypothesis (Supplementary Note 2). If we can exclude the F1
603 hypothesis, we can then subsequently exclude the BC1 hypothesis, despite the similarly
604 noticeable 3:1 ratio observed for hybrid tea roses (74.8% and 25.2% of Asian and European
605 alleles, respectively). To gain a more accurate understanding of the 19th-century rose
606 breeding history, especially concerning the number of generations leading to the "star
607 varieties" in our study, additional research reconstructing pedigrees based on a larger
608 number of whole-genome sequenced accessions will be needed.
609
610
611 **Genetic diversity erosion**
612
613 Nucleotide diversity was estimated over non-overlapping 100-kbp sliding windows on
614 the four groups (namely, ancient European, ancient Asian, early European x Asian and
615 hybrid tea roses), each containing to 16 complete chromosome sets after considering the
616 inferred ploidy based on the distribution of allele balance (Table S2, *e.g.* in Ancient Asian the
617 16 complete chromosome sets corresponds to 6 individuals inferred as diploid individuals,
618 plus a tetraploid). Among all the dataset, the genetic diversity in roses was relatively high
619 with an average π of 1.47×10^{-2} (Fig. 2D). Significant differences in diversity were observed
620 between groups, with higher diversity in the ancient European (1.67×10^{-2}) than in the ancient
621 Asian samples (1.20×10^{-2}).

The “early European x Asian” group exhibits an averaged nucleotide diversity of $1.52x10^{-2}$, a value that slightly exceeds the expectation assuming both the previous estimates and the genetic makeup of this group (50.1%/49.1%, expectation: $1.43x10^{-2}$). This slight burst of genetic diversity in the first generations of hybridization could be explained by the mixing of parental alleles from the two quite divergent genetic backgrounds.

The hybrid tea group has a low nucleotide diversity (average $\pi_{observed}=1.21x10^{-2}$; Fig. 2D), a level that is roughly similar to those of the Asian background ($\pi_{observed}=1.20x10^{-2}$). This diversity is much lower than expected assuming the inferred genomic composition (74.8% Asian, 25.2% European, $\pi_{expected}=1.32x10^{-2}$), corresponding to an average Reduction of Diversity index (RoD) of 8.1%. Given that this breeding history occurred in Europe and that hybrid tea roses have then been preferred to the early European x Asian hybrids in the gardens of residential homes, the evolution between hybrid tea roses and the other European groups is informative about the genetic loss during this period. Comparing these two groups, hybrid teas exhibit an important reduction of diversity as compared to the early European x Asian roses (average RoD=18.5%) and even more as compared to the ancient European accessions (average RoD=27.5%). One could argue that hybrid teas were exported worldwide, including in Asia and therefore that this history of selection could have contributed to an increase of the genetic diversity in Asia. Considering this hypothesis, we compared ancient Asian and hybrid teas and observed such a potential - albeit marginal - gain (RoD= -1.04%). Our results are therefore overall consistent with a net and rapid erosion of nucleotide diversity in Europe during the rose breeding of the 19th century.

The pattern of reduction of diversity between groups is consistent across the chromosomes, even if it varies in intensity (Fig. S11). Comparing the diversity of hybrid teas as compared to ancient European roses, 2.3% of the windows exhibit a reduction of at least half of the diversity (105 among 4,628 windows with RoD exceeding 50%), a value that appears particularly strong given the extremely limited number of generations (Fig. 2C). The maximum observed RoD value on a window is 87.3%, but corresponds to an unanchored scaffold (Chr00) and should therefore be interpreted cautiously. The maximum value for a window anchored on a chromosome is 77.4% (Chr6: 11.2-11.3 Mb). Among the 60 windows with a ROD>0.5 and that are not located on unanchored scaffolds, 35% (21) and 43% (26) are located on chromosomes 3 and 5, respectively, suggesting that these two chromosomes were particularly targeted by artificial selection.

Detecting local genomic footprints of artificial selection

To know more about the history of rose breeding, we investigated how the genomic landscapes of diversity and Tajima’s D have evolved during the rose breeding history (Fig. 3). All landscapes of nucleotide diversity are highly correlated between groups (Fig. S12), even those of the ancient European and ancient Asian groups (Pearson's r=0.301, $p=3.57e^{-87}$). However, the Tajima’s D landscapes of these two groups are independent (Pearson's r=-0.02, p=0.20), suggesting that the correlations of the genomic landscape of diversity are not associated with similar selection targets, but rather more likely shaped by some long-term shared genomic features (*e.g.* the recombination landscape, Shang *et al.,* 2023). The genomic landscapes of diversity become more and more correlated with time, especially when compared to the ancient Asian background (ancient Asian vs. early European x Asian samples, Pearson's r=0.408, $p=1.44e^{-165}$; ancient Asian vs. hybrid tea samples, Pearson's, r=0.566, p=0). Consistently, the Tajima’s D landscapes of the hybrid tea

670 is more correlated with the one of the ancient Asian (Pearson's, r=0.339, p9.26e^{-112}) than
671 with the one of ancient European samples (Pearson's, r=0.170, p=2.70e^{-28}). However the
672 high level and significance of the latter correlation also suggest that artificial selection also
673 targeted alleles from European origin in some genomic regions.
674 Interestingly, the genomic landscapes of nucleotide diversity and Tajima's D are
675 significantly correlated in ancient European (Pearson's r=0.061, p=9.78e^{-5}), as well as in
676 ancient Asian samples (Pearson's r=0.430, p=2.79e^{-185}). However this correlation largely
677 differs in intensity between the two groups. This result is consistent with the lower diversity
678 (Fig. 2D) and the larger variance in Tajima's D in the ancient Asian group (Fig. S13). All
679 together, these results suggest that ancient Asian samples were more impacted by artificial
680 selection prior to their use in the European plant breeding programs than the ancient
681 European samples. Our genomic evidence could be interpreted with regards to the
682 documented knowledge of the long-term history of rose cultivation in China. Chinese roses
683 have been widely cultivated since the Han Dynasty, and selection is known to have occurred
684 during this period, at least for some important traits, including the extension of the flowering
685 period.
686 In order to identify some local genomic footprints of selection, we used hybrid tea
687 roses as references. Indeed, given the limited number of generations of breeding detected
688 (Fig. 2C), the use of hybrid teas allows us to maximize the probability of identifying local
689 footprints of artificial selection. Hybrid tea genomes were scanned for windows exhibiting a
690 shared signal of (i) low π, (ii) negative Tajima's D and (iii) high RoD $\pi_{Hybrid\ Tea}$ *vs.* either π_{Asian}
691 or $\pi_{European}$ (Fig. 3; see Materials & Methods for details). Eighteen windows were detected
692 using the most stringent criteria (last centile of the three metrics, purple lines in Fig. 3),
693 including 15 on a 4-Mb region of the chromosome 3 (from 24.1 and 28.2 Mb, see Table S4).
694 This region is in the immediate vicinity of a previously characterized 5Mb-inversion
695 containing the *RoKSN* gene (28.8 - 33.1 Mb, Kawamura *et al.* 2022), a presumably main
696 target breeding to obtain recurrent-blooming roses with an extended period of blooming. In
697 addition, to these 18 windows, we detected 81 additional windows (last five centiles of the
698 three metrics, pink lines in Fig. 3). Remarkably, five of these additional windows are located
699 at the very end of the inversion (32.5 - 33.1Mb, see Table S4), therefore providing additional
700 support that this footprint is associated with the artificial selection of Asian alleles at *RoKSN*.
701 In the immediate vicinity of the inversion, we find also an homologue of *AP2/TOE*
702 (RC3G0243000, 33.2Mb), another crucial gene controlling the double flower phenotype and
703 therefore partly the number of petals (François *et al.,* 2018; Hibrand-Saint Oyant *et al*.,
704 2018). However, *AP2/TOE* is unlikely to be the gene responsible for this footprint (see
705 Supplementary Note 1), suggesting that recurrent-flowering alleles of RoKSN were the main
706 targets of artificial selection. The three additional windows detected using the most stringent
707 filtering criteria are located on chromosome 5 (two adjacent windows, between 22.9 and 33.1
708 Mb) and on chromosome 1 (33.6-33.7 Mb, Table S4). Most of the additional regions based
709 on the less stringent criteria (last five centiles, see Table S4) are consistent with these three
710 previously detected genomic regions (*i.e.* on chromosomes 1, 3 and 5), but also highlighted
711 a fourth region on chromosome 7 (11 windows between 15.9 and 21.1 Mb, Fig. 3 and Table
712 S4).
713
714
715

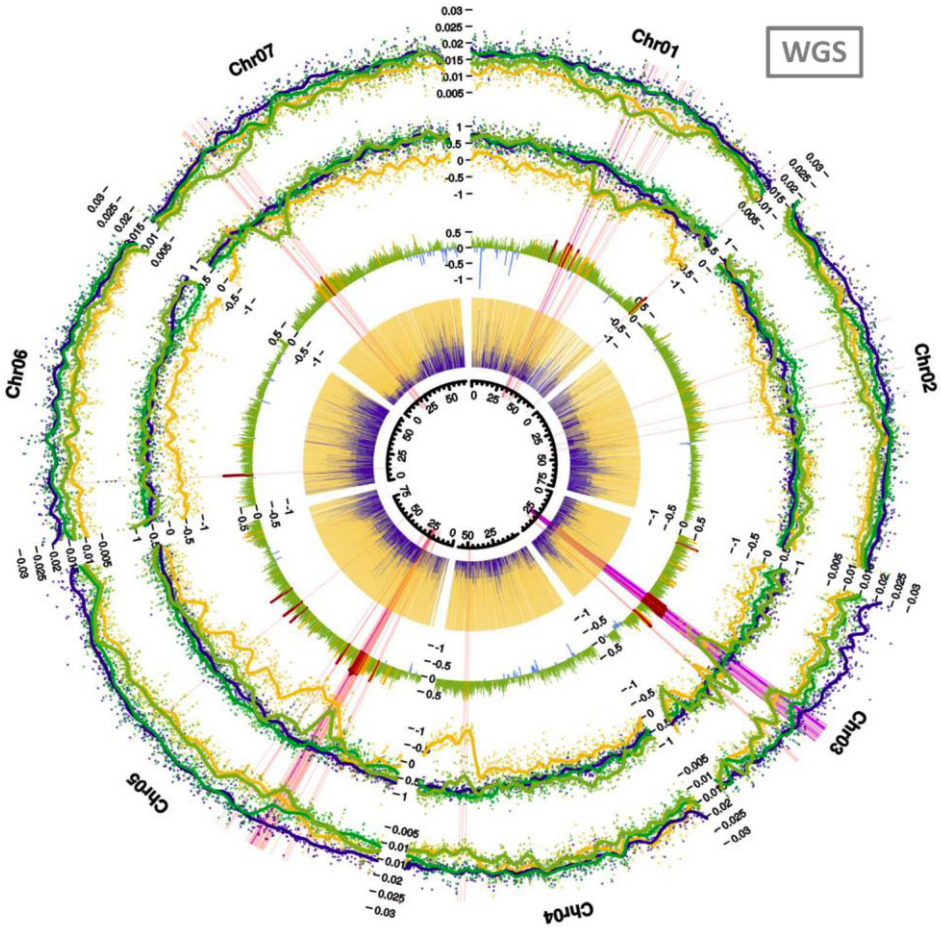

716
717 ***Fig. 3: Detection of regions exhibiting footprints of artificial selection in hybrid tea***
718 ***roses.*** *From external to internal: nucleotide diversity, Tajima's D, RoD* $_{Hybrid\ tea\ vs.\ Ancient\ European}$,
719 *and local ancestry as estimated at diagnostic SNPs. Blue and yellow refer to ancient*
720 *European and ancient Asian backgrounds respectively, while dark and light green refer to*
721 *early European x Asian and hybrid tea groups, respectively. Pink and purple lines*
722 *correspond to windows that simultaneously exhibit one of the lowest nucleotide diversity*
723 *(bottom 5% or bottom 1%, respectively), one of the lowest Tajima's D (bottom 5% or bottom*
724 *1%, respectively) and one of the highest RoD (either in* $RoD_{European\ vs.\ Hybrid\ tea}$ *or* $RoD_{Asian\ vs\ Hybrid\ tea}$, *top 5% or top 1%, respectively). Results from chr00 (corresponding to all*
726 *unanchored scaffolds in Hibrand-Saint Oyant et al., 2018) are not shown.*
727
728
729 **The largest rose GWAS catalog to date**
730
731 In addition to reconstructing the history of rose breeding, we conducted a large
732 Genome-Wide Association Study (GWAS) with the aim of identifying associations between
733 the genotypes at the 204 varieties and the different phenotypes. Given the large number of
734 phenotypes we investigated, as well as the variety of scenarios possible regarding
735 dominance in polyploids (Rosyara *et al.,* 2016), a dedicated website portal has been created
736 in order to explore all the results (hereafter referred to as the rose GWAS browser,
737 https://roseGWASbrowser.github.io/). The online browser allows to select a category of traits
738 (*e.g.* petal counts or colors, plant architecture, scent), then a specific trait (*e.g.* 2-
739 phenylethanol content), and select a specific scenario regarding the polyploid gene action,

among additive, simplex dominant and duplex dominant scenarios. For some traits, the GWAS explorer not only reports the results of the GWAS when the trait was analyzed quantitatively, but also when analyzed qualitatively, which can be meaningful when distribution of the trait values are more bimodally distributed.

The rose GWAS explorer is a tool designed to accelerate research on rose breeding. As a textbook example, we have decided to focus on the identification of genomic regions that correlated with the resistance to the blackspot disease, which is one of the most impactfuldiseases in garden roses. To identify some regions, we performed GWAS for three years of scoring (Fig. 4, see also Fig. S14). The number of significantly associated SNPs greatly vary depending on the year of scoring (red dots, Fig. 4). The relative lack of resolution is likely associated with the difficulty of performing GWA studies in populations for which phenotypes still highly correlate with the population structure gradient as a result of the limited number of generations (*e.g.* see Fig. S4). Indeed, similar results were observed for most of the investigated traits. As a consequence, all the results should be interpreted with some caution, requiring further validation through independent analyses. Here, some potential genomic regions of interest are detected, including a genomic region at the very end of chromosome 4 that is associated with the three years of scoring. Additional locations are also observed on chromosome 3 for some of the years, including in a region that collocates with a meta-QTL recently identified in three different experimentally segregating populations, which were phenotyped for black spot disease over several years and locations (Lopez Arias *et al.* 2020).

Discussion

Evolution of the genetic diversity in roses

Genetic diversity is one fundamental unit of biodiversity since sufficient within-species diversity is needed to face different threats, including diseases, pests, changes in climate, as well as more intrinsic factors associated with evolution under low effective population sizes, and therefore reduce mid- and long-term extinction risks. In December 2022, as part of the United Nations Biodiversity Conference (COP15), the post-2020 framework of the Convention on Biological Diversity was enacted (CBD, 2022). Among the four goals and 23 targets, the adopted framework includes central ambitions regarding the maintenance and the restoration of the genetic diversity in wild species, but also in domesticated species, in order to safeguard their adaptive potential (Goal A & Target 4). The reduction of diversity of domesticated species has often been viewed as a less vital topic as compared to the preservation of wild species. The recent report of a sharp reduction of the genetic diversity in bread wheat, with a loss of diversity of around 30% over the 20th century (Pont *et al.,* 2019), should make us question the potential consequences regarding the worldwide food security, given the central importance of cereals in the human and domesticated animal diet.

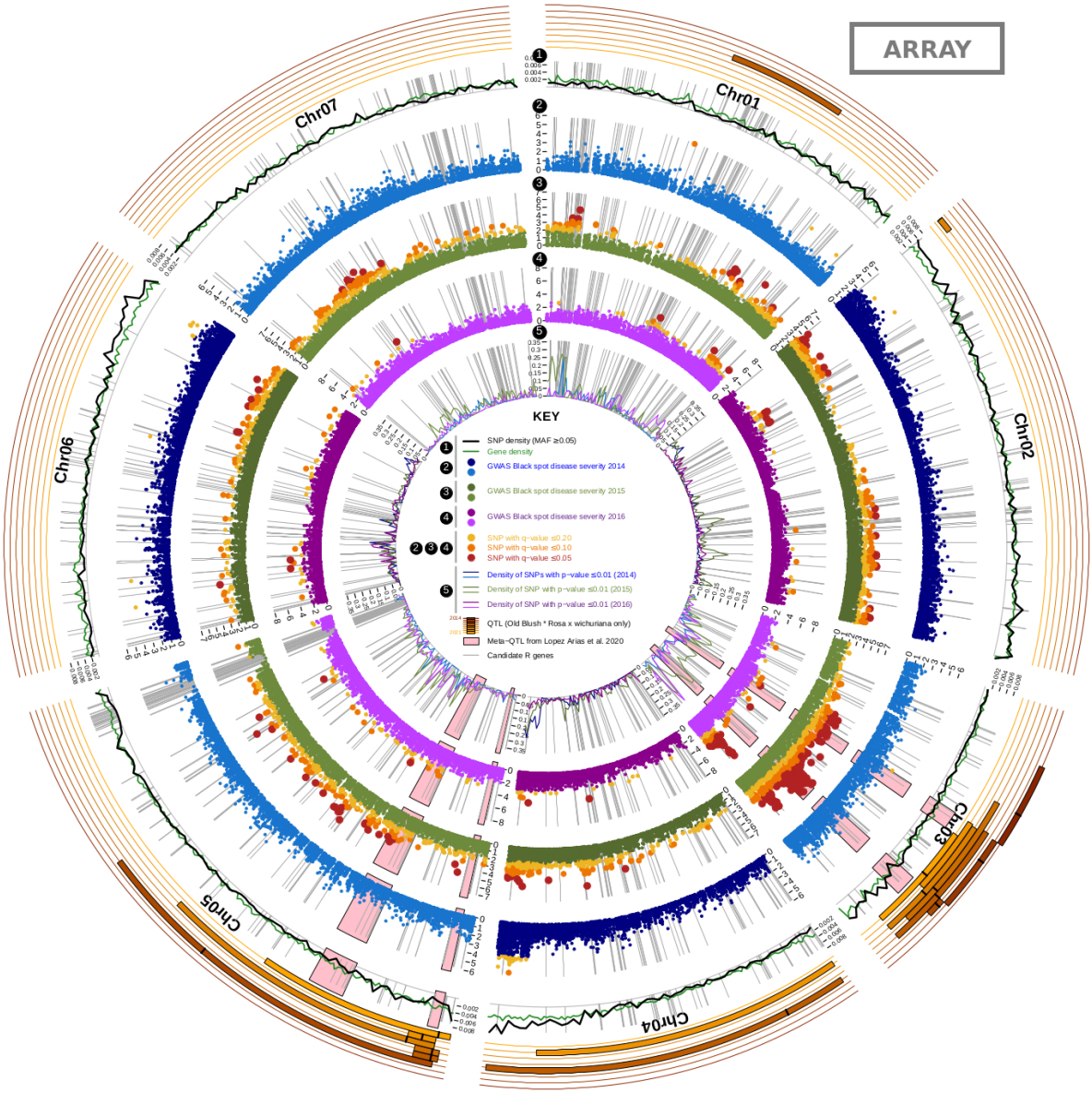

Figure 4: GWAS for black spot resistance. *1: Per-window SNP array density and gene density based on the reference genome (Hibrand-Saint Oyant et al., 2018). 2-4: Manhattan plots of the p-values along the genome for the three years of scoring (2: 2014, 3: 2015, 4: 2016) under the general model of GWASpoly. SNPs with q-values < 0.20, 0.10 and 0.05 are shown in yellow, orange and red, respectively. 5: Local density in highly associated SNPs (p-value < 0.01) for each of the three years of scoring (2014, 2015 and 2016 are shown with blue, green and purple lines). QTLs and metaQTLs from Lopez-Arias et al., 2020 based on three segregating populations (connected by male resistant parent Rosa x wichurana) are also shown. The candidate R genes correspond to an expert annotation of NBS-LRR encoding genes (Lopez-Arias et al., 2020). Results for SNPs located on chr00 (corresponding to all unanchored scaffolds in Hibrand-Saint Oyant et al., 2018) are not shown here (but see Fig. S14 for non-circular Manhattan plots of the p-values including chr00).*

In the present study, we have questioned how the genetic diversity has evolved during the 19th century, a century corresponding to the golden age for European rose breeding, with an exploding number of varieties (estimated to be around 100 in 1800 and to be 8,000 in 1900; Marriott, 2003, Oghină-Pavie, 2021). Our result is consistent with a substantial reduction of diversity, of around 27.5% in a century in Europe (Fig. 2D), comparing the ancient European and the hybrid tea roses. This reduction has taken place across a very limited number of generations (< 10, Fig. 2C) and is associated with both the backcrossing with a pre-selected Asian genetic background (Figs. 2 & S6-9) and with additional footprints of artificial selection (Fig. 3).

Despite that this observed reduction of genetic diversity could be considered as more minor regarding a horticultural species as compared to a crop species such as bread wheat, it still holds implications for humans. Indeed, roses represent a common heritage of mankind and serves as a significant cornerstone in the ornamental sector (more than 10 billion dollars, Feng et al, 2022), in addition to being used as a source of food and medicine in some societies. In roses, grafting however makes the long-term maintenance of ancient varieties possible, allowing the backcrossing of modern varieties, improved regarding some specific traits, with more ancient and genetically diverse varieties. This restoration of this genetic diversity is however only possible if the ancient garden roses are maintained over the long term. In roses, two main action targets should be therefore proposed: (i) increasing effort, especially regarding state funding, for safeguarding gardens containing botanical and ancient varieties, and (ii) alert the stakeholders of the importance of maintaining and restoring the genetic diversity in order to ensure a sustainable breeding for long-term, which could be associated with new future breeding targets (*e.g.* new emerging diseases, anthropogenic disturbances or ecosystemic services in urban areas).

Looking back in time to identify selection targets

Another tremendous advantage of the use of grafted garden roses as domesticated plant models is our ability to phenotype varieties bred during more than a century all together at the same time in a common rose garden. Phenotypically, we indeed have reported important temporal changes in the number of petals, the ability of roses to bloom several times in a year and the susceptibility to the black spot disease (Fig. 1), even if the latter trait evolution was likely unintended. The temporal increase in the number of petals is relatively continuous until 1870, before a slight reduction on average, which seems more associated with the progression toward a bimodal distribution for this specific trait and questions the diversification of the consumer tastes at that time, including the return to simple flowers for some varieties (Fig. 1; see also Oghina-Pavie, 2020). Roses of a given period should not be considered as a homogeneous ensemble, they are rather representative of different tastes and breeding objectives among breeders, in such a way that the history of breeding should not be oversimplified. Similarly to petal counts, the susceptibility to black spot has increased until 1890, before a reduction on average, again associated with a marked bimodal distribution (Fig. 1).

The extension of the flowering period by selecting recurrent blooming varieties was often assumed to be the main target of selection during the 19th century. Consistently, during this period, we indeed observed a continuous increase of an index that measures the ability of a rose to rebloom (Fig. 1). Such a continuous selection has likely contributed to

generate a marked footprint of selection in rose genomes, since the sharpest signature of the selective sweep is observed above one of the two breaking points of a previously characterized 5-Mb inversion of the *RoKSN* gene (chromosome 3, 28.8 - 33.1 Mb, Hibrand-Saint Oyant *et al.,* 2018; Kawamura *et al.,* 2022). Consistent signal was also observed at the second breaking point (Fig. 3), in agreement with the selection in this region. Several alleles at the *RoKSN* gene leading to the extended period were described, including a $RoKSN^{copia}$ and a $RoKSN^{NULL}$. Previously, it was demonstrated a progressive selection of the $RoKSN^{copia}$ allele during the 19th century (Soufflet-Freslon *et al.,* 2021). This allele is not present in the reference genome we used, this genome contains a large rearrangement at the *RoKSN* locus leading to the $RoKSN^{NULL}$ allele (Hibrand-Saint Oyant *et al.,* 2018). This rearrangement may explain the complexity of the local footprints associated with the nucleotide diversity and Tajima's D landscapes. Additional footprints have been also uncovered, but currently were not associated with any previously reported genes. In the future, thanks to more numerous whole-genome sequences available, as well as the new technological and methodological developments allowing the access to phased polyploid genomes, a much clearer picture could be anticipated. Extending these investigations to the 20th century could be of particular interest since more modern roses are characterized by a clearer distinction between the genetics used for garden *vs.* cut roses. Cut roses - especially red ones - have potentially experienced a more intense reduction of global genetic diversity and more pronounced local footprints of selection, as typical expected based on the huge difference of the two respective markets (*e.g.* in France in 2018, garden roses: 50M€, cut roses: 376M€, Clotault et al. 2022).

Advances and challenges for GWAS in rose

As a tool for the future of rose breeding, we have released the largest GWAS catalog for rose (https://roseGWASbrowser.github.io/). Our GWAS browser allows the website visitors to explore the association with more than 25 traits, on the basis of our panel of 204 accessions. The objective is to make future breeding more effective for some traits, including the resistance to the black spot disease (Fig. 4). This trait represents a typical example of an important target need in order to find sources of genetic resistances in roses, in the context of a tightening environmental legislation associated with the use of chemicals due to their deleterious environmental impacts and health risks.

Despite the great advance made with the release of the GWAS catalog, the direct insights appear relatively limited to date. Indeed, the GWAS strategy in our panel has generated few repeatable and easily interpretable signatures of associations. As compared with the use of QTL mapping in experimental crosses, extensive GWAS analyses seem to have a more limited benefit in rose than on some other domesticated or non-domesticated species (*e.g.* Korte & Farlow, 2013; Alqudah *et al.,* 2020). Several non-mutually exclusive reasons could explain this paradox: (i) a too limited number of varieties used in our study, (ii) the limited number of generations of recombination in the investigated collection (Fig. 2C) that could contribute to maintaining a predominant association with the population structure, leading to a low statistical power in the model. Combining GWAS and QTL approaches (Fig. 4), when available, offers the possibility to increase the statistical support for some regions of interest, extends the allelic diversity by considering other alleles than those segregating between the parents, describes the genomic locations of the associated regions and prioritizes the research effort. As a typical example, the last third of chromosome 3 could

appear as a more promising region for selection, therefore guiding the research efforts in this direction. Remarkably, chromosome 3 has been associated with many traits in rose (resistance to black spot, but also number of petals, fragrance, prickles, recurrent blooming, self-incompatibility; *e.g.* Hibrand-Saint Oyant *et al.,* 2018, Kawamura *et al.,* 2022), which could therefore suggests the presence of tradeoffs between some traits of interest. A more detailed genomic characterization of the genomic landscapes, including local linkage disequilibrium patterns, based on more modern varieties, isespecially needed on this chromosome.

Conclusion

Combining large phenotypic data and genetic investigations using 204 individuals genotyped using a high density SNP array, plus 32 whole-genome sequences, we found support for both phenotypic and genomic changes during the 19th century. With an unprecedented accuracy, we confirmed the progressive shift from a European to a more Asian-like genetic background, with Hybrid tea roses exhibiting a three-quarter Asian genetic background. This genetic makeup likely corresponds to several generations of backcrossing of the early European x Asian varieties with the ancient genetic background, as it was previously suggested (Liorzou *et al.,* 2016, see also Supplementary Note 2). As a result of the lower resident diversity in the ancient Asian varieties, partly due to a more ancient and intense history of selection in Asia, as well as to some specific genomic footprints of artificial selection - especially in the region of *RoKSN* -, rose breeding in Europe has contributed to a substantial loss of genetic diversity during the 19th century (up to 27.5% in hybrid tea roses). In addition to providing a fine description of the history of rose breeding, we have generated the largest GWAS catalog to date, with the aim of providing fundamental knowledge for the future of rose breeding.

Acknowledgments

This research was conducted in the framework of the regional programme "Objectif Végétal, Research, Education and Innovation in Pays-de-la-Loire“, supported by the French Region Pays-de-la-Loire, Angers Loire Métropole and the European Regional Development Fund. A part of the phenotypic data was supported by the FLORHIGE (French Region Pays-de-la-Loire), the SIFLOR (BAP division of INRAE) and Rosascent projects (ANR, grant number ANR-16-CE20-0024-01). We acknowledge the Roseraie Loubert (Gennes-Val-de-Loire, France) and Biological Resource Center Pome Fruits and Roses (Angers, France) for maintaining the genetic resources and their associated data. We also acknowledge the Gentyane facility (INRAE Clermont-Ferrand, France) and the ANAN platform of the SFR Quasav (Angers, France; including Muriel Bahut) for the genotyping data. Thibault Leroy is also grateful to the university of Vienna, Austria for its financial support regarding the whole-genome sequencing of the rose varieties. We would like to thank the Next Generation Sequencing Facility at Vienna BioCenter Core Facilities (VBCF), member of the Vienna BioCenter (VBC), Austria. We are grateful to the genotoul bioinformatics platform Toulouse Occitanie (Bioinfo Genotoul, https://doi.org/10.15454/1.5572369328961167E12) for

providing computing and storage resources. We also thank Jérôme Chené (Pépinières Roses Loubert, Gennes-Val-de-Loire, Pays-de-la-Loire, France) for providing fresh plant material of a few whole-genome resequenced individuals. We also thank Roeland Voorrips and Giorgio Tumino for their valuable advice regarding fitPoly and GWASpoly at the beginning of the project.

Competing interests

The authors declare no competing interest. Although E.A. is a Syngenta seeds SAS employee, her contribution to the project predates her recruitment by the company and does not pertain to her current activities or the interests of the company.

Author contributions

T.Le., E.A., S.B., J-C.C., C.O.P, F.F., L.H.S.O & J.Cl. designed research; T.Le., E.A., T.T., A.C, J.Ch, T.Lo., A.P., V.S.F, F.F., L.H.S.O & J.Cl contributed to the sampling; A.C. & L.H.S.O. performed DNA extractions; J.J. performed the *RoKSN* and *RoAP2 genes* genotyping; T.T., J.C., T.Lo., A.P. & V.S.F contributed to the phenotyping; S.B., J-C.C. & S.N.P. contributed to the GC-mass spectrometry data; T.Le & E.A. analyzed data under the supervision of C.O.P, F.F., L.H.S.O. & J.Cl.; T.Le. drafted the manuscript. All authors have subsequently read, edited and approved the manuscript.

Data availability

Raw sequencing data of the newly sequenced roses are publicly available on the Sequence Read Archive (SRA) under the BioProject PRJNA997103. Scripts were made available on github: https://github.com/roseGWASbrowser/PopGen_GWAS_19thcentury_roses. The GWAS rose browser is available at https://roseGWASbrowser.github.io.

References

Allaby RG, Ware RL, Kistler L. 2019. A re-evaluation of the domestication bottleneck from archaeogenomic evidence. *Evolutionary Applications* 12: 29–37.

Alqudah AM, Sallam A, Stephen Baenziger P, Börner A. 2020. GWAS: Fast-forwarding gene identification and characterization in temperate Cereals: lessons from Barley – A review. *Journal of Advanced Research* 22: 119–135.

Altman A, Shennan S, Odling-Smee J. 2022. Ornamental plant domestication by aesthetics-driven human cultural niche construction. *Trends in Plant Science* 27: 124–138.

983 Augusto Corrêa Dos Santos R, Goldman GH, Riaño-Pachón DM. 2017. ploidyNGS: visually
984 exploring ploidy with Next Generation Sequencing data. *Bioinformatics (Oxford, England)* 33:
985 2575–2576.

986 Bergougnoux V, Caissard J-C, Jullien F, Magnard J-L, Scalliet G, Cock JM, Hugueney P,
987 Baudino S. 2007. Both the adaxial and abaxial epidermal layers of the rose petal emit
988 volatile scent compounds. *Planta* 226: 853–866.

989 Bolger AM, Lohse M, Usadel B. 2014. Trimmomatic: a flexible trimmer for Illumina sequence
990 data. *Bioinformatics (Oxford, England)* 30: 2114–2120.

991 Brown TA. 2019. Is the domestication bottleneck a myth? *Nature Plants* 5: 337–338.

992 Caissard J-C, Adrar I, Conart C, Paramita SN, Baudino S. 2023. Do we really know the scent
993 of roses? *Botany Letters* 170: 77–88.

994 Chowdhuri TK, Deka K. 2019. Biodiversity and Conservation of Ornamental Crops.
995 *Conservation and Utilization of Horticultural Genetic Resources*.

996 Clotault J, Foucher F, Grapin A, Hibrand-Saint Oyant L, Malécot V, Paillard S, Pernet A,
997 Soufflet-Freslon V, Oghina-Pavie C. 2022. Rose selection in France: a long and beautiful
998 history. *Chronica Horticulturae* 62: 28–37.

999 Convention on Biological Diversity. 2022. COP15: Final text of Kunming-Montreal Global
1000 Biodiversity Framework.

1001 Csárdi G, Nepusz T. 2006. The igraph software package for complex network research.

1002 Debray K, Le Paslier M-C, Bérard A, Thouroude T, Michel G, Marie-Magdelaine J, Bruneau
1003 A, Foucher F, Malécot V. 2022. Unveiling the Patterns of Reticulated Evolutionary Processes
1004 with Phylogenomics: Hybridization and Polyploidy in the Genus Rosa. *Systematic Biology*
1005 71: 547–569.

1006 Diamond J. 2002. Evolution, consequences and future of plant and animal domestication.
1007 *Nature* 418: 700–707.

1008 Diamond JM. 2005. *Guns, germs, and steel: the fates of human societies*. New York: Norton.

1009 Ducomet, V. 1903. Une maladie des feuilles du Rosier *Marsonia Rosae* Briosi et cav. in Le
1010 Jardin: 199.

1011 François L, Verdenaud M, Fu X, Ruleman D, Dubois A, Vandenbussche M, Bendahmane A,
1012 Raymond O, Just J, Bendahmane M. 2018. A miR172 target-deficient AP2-like gene
1013 correlates with the double flower phenotype in roses. *Scientific Reports* 8: 12912.

1014 Gattolin S, Cirilli M, Pacheco I, Ciacciulli A, Da Silva Linge C, Mauroux J-B, Lambert P,
1015 Cammarata E, Bassi D, Pascal T, *et al.* 2018. Deletion of the miR172 target site in a TOE-
1016 type gene is a strong candidate variant for dominant double-flower trait in Rosaceae. *The*
1017 *Plant Journal* 96: 358–371.
1018
1019 Gaut BS, Díez CM, Morrell PL. 2015. Genomics and the Contrasting Dynamics of Annual
1020 and Perennial Domestication. *Trends in Genetics* 31: 709–719.

1021 Gessert G. 1993. Flowers of Human Presence: Effects of Esthetic Values on the Evolution of
1022 Ornamental Plants. *Leonardo* 26: 37–44.

1023 Gessert G. 2010. *Green Light: Toward an Art of Evolution*. The MIT Press.

1024 Goody J. 1993. *The Culture of Flowers*. Cambridge University Press.

1025 Gu Z, Gu L, Eils R, Schlesner M, Brors B. 2014. circlize implements and enhances circular
1026 visualization in R. *Bioinformatics* 30: 2811–2812.

1027 Hibrand Saint-Oyant L, Ruttink T, Hamama L, Kirov I, Lakhwani D, Zhou NN, Bourke PM,
1028 Daccord N, Leus L, Schulz D, *et al.* 2018. A high-quality genome sequence of Rosa
1029 chinensis to elucidate ornamental traits. *Nature Plants* 4: 473–484.

1030 Iwata H, Gaston A, Remay A, Thouroude T, Jeauffre J, Kawamura K, Oyant LH-S, Araki T,
1031 Denoyes B, Foucher F. 2012. The TFL1 homologue KSN is a regulator of continuous
1032 flowering in rose and strawberry. *The Plant journal: for cell and molecular biology* 69: 116–
1033 125.

1034 Jombart T. 2008. adegenet: a R package for the multivariate analysis of genetic markers.
1035 *Bioinformatics* 24: 1403–1405.

1036 Kawamura K, Ueda Y, Matsumoto S, Horibe T, Otagaki S, Wang L, Wang G, Hibrand-Saint
1037 Oyant L, Foucher F, Linde M, *et al.* 2022. The identification of the Rosa S-locus provides
1038 new insights into the breeding and wild origins of continuous-flowering roses. *Horticulture*
1039 *Research* 9: uhac155.

1040 Koning-Boucoiran CFS, Esselink GD, Vukosavljev M, van ’t Westende WPC, Gitonga VW,
1041 Krens FA, Voorrips RE, van de Weg WE, Schulz D, Debener T, *et al.* 2015. Using RNA-Seq
1042 to assemble a rose transcriptome with more than 13,000 full-length expressed genes and to
1043 develop the WagRhSNP 68k Axiom SNP array for rose (Rosa L.). *Frontiers in plant science*
1044 6: 249.

1045 Korte A, Farlow A. 2013. The advantages and limitations of trait analysis with GWAS: a
1046 review. *Plant methods* 9: 29.

1047 Korunes KL, Samuk K. 2021. pixy: Unbiased estimation of nucleotide diversity and
1048 divergence in the presence of missing data. Molecular Ecology Resources 21:1359-1368.

1049 Leroy T, Anselmetti Y, Tilak M-K, Bérard S, Csukonyi L, Gabrielli M, Scornavacca C, Milá B,
1050 Thébaud C, Nabholz B. 2021a. A bird’s white-eye view on avian sex chromosome evolution.
1051 *Peer Community Journal* 1.

1052 Leroy T, Rousselle M, Tilak M-K, Caizergues AE, Scornavacca C, Recuerda M, Fuchs J,
1053 Illera JC, De Swardt DH, Blanco G, *et al.* 2021b. Island songbirds as windows into evolution
1054 in small populations. *Current Biology* 31: 1303-1310.e4.

1055 Leus L, Van Laere K, De Riek J, Van Huylenbroeck J. 2018. Rose. In: Van Huylenbroeck J,
1056 ed. Ornamental Crops. Cham: Springer International Publishing, 719–767.

1057

1058 Liorzou M, Pernet A, Li S, Chastellier A, Thouroude T, Michel G, Malécot V, Gaillard S, Briée
1059 C, Foucher F, *et al.* 2016. Nineteenth century French rose (Rosa sp.) germplasm shows a
1060 shift over time from a European to an Asian genetic background. *Journal of Experimental*
1061 *Botany* 67: 4711–4725.

1062 Lopez Arias DC, Chastellier A, Thouroude T, Bradeen J, Van Eck L, De Oliveira Y, Paillard
1063 S, Foucher F, Hibrand-Saint Oyant L, Soufflet-Freslon V. 2020. Characterization of black

spot resistance in diploid roses with QTL detection, meta-analysis and candidate-gene identification. *Theoretical and Applied Genetics* 133: 3299–3321.

Magnard J-L, Roccia A, Caissard J-C, Vergne P, Sun P, Hecquet R, Dubois A, Hibrand-Saint Oyant L, Jullien F, Nicolè F, *et al.* 2015. Biosynthesis of monoterpene scent compounds in roses. *Science* 349: 81–83.

Manichaikul A, Mychaleckyj JC, Rich SS, Daly K, Sale M, Chen W-M. 2010. Robust relationship inference in genome-wide association studies. *Bioinformatics (Oxford, England)* 26: 2867–2873.

Marolleau B, Petiteau A, Bellanger M-N, Sannier M, Le Pocreau N, Porcher L, Paillard S, Foucher F, Thouroude T, Serres-Giardi L, *et al.* 2020. Strong differentiation within Diplocarpon rosae strains based on microsatellite markers and greenhouse-based inoculation protocol on Rosa. *Plant Pathology* 69: 1093–1107.

Marriott M. 2003. Encyclopedia of Rose Science.

Martin M, Piola F, Chessel D, Jay M, Heizmann P. 2001. The domestication process of the Modern Rose: genetic structure and allelic composition of the rose complex. *Theoretical and Applied Genetics* 102: 398–404.

Moyers BT, Morrell PL, McKay JK. 2018. Genetic Costs of Domestication and Improvement. *Journal of Heredity* 109: 103–116.

Nei M, Maruyama T, Chakraborty R. 1975. The bottleneck effect and genetic variability in populations. *Evolution* 29: 1–10.

Oghină-Pavie C. 2020. La raison des rosomanes. Les sciences naturelles dans le Journal des Roses à la fin du XIXe siècle. *Romantisme* 190: 64-78.

Oghină-Pavie C. 2021. Les rosiers et la nouveauté horticole en France au début du XIXe siècle, in J. Baudry, J. Blanc, L. Hilaire-Pérez, M. Ratcliff, S. Wenger (eds), Produire du nouveau ? Arts-techniques-sciences en Europe (1400-1900), Paris, CNRS Éditions: 83-94.

Picard toolkit. 2019. *Broad Institute, GitHub* repository https://broadinstitute.github.io/picard/

Pont C, Leroy T, Seidel M, Tondelli A, Duchemin W, Armisen D, Lang D, Bustos-Korts D, Goué N, Balfourier F, *et al.* 2019. Tracing the ancestry of modern bread wheats. *Nature Genetics* 51: 905–911.

Poplin R, Ruano-Rubio V, DePristo M, Fennell J, Carneiro M, Auwera G, Kling D, Gauthier L, Levy-Moonshine A, Roazen D, *et al.* 2018. Scaling accurate genetic variant discovery to tens of thousands of samples. *bioRxiv*: 201178.

Proïa F, Pernet A, Thouroude T, Michel G, Clotault J. 2016. On the characterization of flowering curves using Gaussian mixture models. *Journal of Theoretical Biology* 402: 75–88.

Purcell S, Neale B, Todd-Brown K, Thomas L, Ferreira MAR, Bender D, Maller J, Sklar P, de Bakker PIW, Daly MJ, *et al.* 2007. PLINK: a tool set for whole-genome association and population-based linkage analyses. *American journal of human genetics* 81: 559–575.

Purugganan MD. 2022. What is domestication? *Trends in ecology & evolution* 37: 663–671.

Raj A, Stephens M, Pritchard JK. 2014. fastSTRUCTURE: variational inference of population structure in large SNP data sets. *Genetics* 197: 573–589.

1104 Raymond O, Gouzy J, Just J, Badouin H, Verdenaud M, Lemainque A, Vergne P, Moja S,
1105 Choisne N, Pont C, *et al.* 2018. The *Rosa* genome provides new insights into the
1106 domestication of modern roses. *Nature Genetics* 50: 772–777.

1107 Roccia A, Hibrand-Saint Oyant L, Cavel E, Caissard J-C, Machenaud J, Thouroude T,
1108 Jeauffre J, Bony A, Dubois A, Vergne P, *et al.* 2019. Biosynthesis of 2-Phenylethanol in
1109 Rose Petals Is Linked to the Expression of One Allele of RhPAAS. *Plant physiology* 179:
1110 1064–1079.

1111 Rosyara UR, De Jong WS, Douches DS, Endelman JB. 2016. Software for Genome-Wide
1112 Association Studies in Autopolyploids and Its Application to Potato. *The Plant Genome* 9:
1113 plantgenome2015.08.0073.

1114 Schulz DF, Schott RT, Voorrips RE, Smulders MJM, Linde M, Debener T. 2016. Genome-
1115 Wide Association Analysis of the Anthocyanin and Carotenoid Contents of Rose Petals.
1116 *Frontiers in plant science* 7: 1798.

1117 Shang H, Field DL, Paun O, Rendón-Anaya M, Hess J, Vogl C, Liu J, Ingvarsson PK, Lexer
1118 C, Leroy T. 2023. Drivers of genomic landscapes of differentiation across a *Populus*
1119 divergence gradient. *Molecular Ecology*, in press.

1120 Slowikowski K. 2023. ggrepel: Automatically Position Non-Overlapping Text Labels with
1121 'ggplot2'.

1122 Smith O, Nicholson WV, Kistler L, Mace E, Clapham A, Rose P, Stevens C, Ware R,
1123 Samavedam S, Barker G, *et al.* 2019. A domestication history of dynamic adaptation and
1124 genomic deterioration in Sorghum. *Nature Plants* 5: 369–379.

1125 Soufflet-Freslon V, Araou E, Jeauffre J, Thouroude T, Chastellier A, Michel G, Mikanagi Y,
1126 Kawamura K, Banfield M, Oghina-Pavie C, *et al.* 2021. Diversity and selection of the
1127 continuous-flowering gene, RoKSN, in rose. *Horticulture Research* 8: 76.

1128 Spiller M, Berger RG, Debener T. 2010. Genetic dissection of scent metabolic profiles in
1129 diploid rose populations. *Theoretical and Applied Genetics* 120: 1461–1471.

1130 Turner S. 2018. qqman: an R package for visualizing GWAS results using Q-Q and
1131 manhattan plots. Journal of Open Source Software 3:731

1132 Vasimuddin M, Misra S, Li H, Aluru S. 2019. Efficient Architecture-Aware Acceleration of
1133 BWA-MEM for Multicore Systems. In: 314–324.

1134 Voorrips R.E., Gort G. Vosman B. 2011. Genotype calling in tetraploid species from bi-allelic
1135 marker data using mixture models. BMC Bioinformatics 12, 172.
1136
1137 Wickham H. 2016. *ggplot2: Elegant Graphics for Data Analysis*. Springer-Verlag New York.

1138 Wissemann V, Ritz CM. 2007. Evolutionary patterns and processes in the genus Rosa
1139 (Rosaceae) and their implications for host-parasite co-evolution. *Plant Systematics and*
1140 *Evolution* 266: 79–89.

1141 Zheng X, Levine D, Shen J, Gogarten SM, Laurie C, Weir BS. 2012. A high-performance
1142 computing toolset for relatedness and principal component analysis of SNP data.
1143 *Bioinformatics (Oxford, England)* 28: 3326–3328.